Torsional Negative Stiffness Mechanism for Bidirectional Morphing Aircraft Actuation

Jiaying Zhang[1,*], Alexander D. Shaw[1], Mohammadreza Amoozgar[1], Michael I. Friswell[1] and Benjamin K.S. Woods[2]

[1] College of Engineering, Swansea University, Swansea SA1 8EN, United Kingdom

[2] Department of Aerospace Engineering, University of Bristol, Bristol BS8 1TR, United Kingdom

[*]E-mail: jiaying.zhang@swansea.ac.uk

Abstract. Traditional morphing concepts require external energy input to achieve the desired changes to the shape of aircraft structures, often working against the inherent stiffness of these structures. This can lead to a requirement for large actuators, and a significant negative impact on system level performance due to the added mass and energy requirements. This work investigates an energy efficient concept for bidirectional morphing aircraft actuation by using a negative stiffness mechanism. The negative stiffness mechanism reduces the actuation requirements for morphing structures by strategically locating negative stiffness devices in parallel to the positive stiffness of the morphing structure to create a net zero stiffness system and therefore to tailor the required deployment forces and moments with minimal energy requirements. The torsional negative stiffness with an off centre spring (TNSOCS) mechanism proposed here uses a pre-tensioned spring to convert the decreasing spring force available in the spring into increasing output balanced torque. The kinematics of the negative stiffness mechanism is first developed to achieve bidirectional actuation and its geometry is then optimised by employing an energy conversion efficiency function. The performance of the optimised negative stiffness mechanism is evaluated through net torque, the total required energy and energy conversion efficiency. Exploiting the negative stiffness mechanism has a significant benefit not only in the field of morphing aircraft but many other energy sensitive applications.

1. Introduction

Traditional aircraft structures are designed with actuated substructures connected with discrete mechanical elements for adapting to different flight conditions with corresponding targets or requirements during flight. These designs can add significantly to the mass and requirements for the design, manufacture and maintenance, which adversely influence the flight performance and energy consumption at the aircraft system level. Morphing aircraft seek to remedy this by integrating actuation into the structures themselves to achieve simplicity and efficiency to improve flight performance and energy efficiency. Many works on morphing structures have been presented, including modelling, devices and challenges [1–4].

Different approaches have been investigated to actuate morphing aircraft. Some general actuators have been used to accomplish chord extension [5], wing area and sweep angle change [6], profile adjustment [7] and morphing winglet deployment [8,9]. These integrated systems allow shape changes of the structure, and thus controlling its motion with acceptable precision. Traditional actuators, such as electromechanical actuation, can be used as linear and rotary actuators, combined with mechanisms to provide a powerful tool for morphing [10]. Moreover, with the development of smart materials, many traditional actuation systems based on electric motors, hydraulics, or pneumatics may be replaced by smart material systems. For example, piezoelectric materials have been used as actuators to control wing panels [11,12], spanwise deflection [13] and trailing-edge flaps [14,15]. Other smart materials have been investigated for morphing structures [2,16,17], based on electric, magnetic or thermal activation, which gives enormous benefits to the actuation system, such as high energy density [18,19]. These different methods are able to morph the aircraft, but the energy required is dependent on external actuators, which can have a significant negative impact on the system level performance due to the added mass and high energy requirements. Therefore, minimising this external energy input can be the key to optimising morphing aircraft at the system level.

The objective of this paper is to reduce the required energy for bidirectional morphing aircraft actuation by establishing an energy balancing system. The key concept is developing an additional negative stiffness system to balance the positive stiffness morphing system. Although the concept of using negative stiffness has been investigated to achieve stiffness changes in a dynamic system [20,21], the alternative use of negative stiffness systems can be beneficial for statically balanced systems such as morphing aircraft. Previously, Woods et al. used a spiral shaped pulley to tailor the actuation force from a pneumatic actuator [22,23]. Through the kinematic tailoring, the output load line can be well matched the required torque to drive a compliant morphing aircraft. An experiment validated the approach using two springs (drive spring and load spring) [24]. Figure 1 shows the 3D printed spiral pulley negative stiffness mechanism, which uses a prearranged extension spring as the drive spring to tailor the required load, that represents the morphing aircraft actuation.

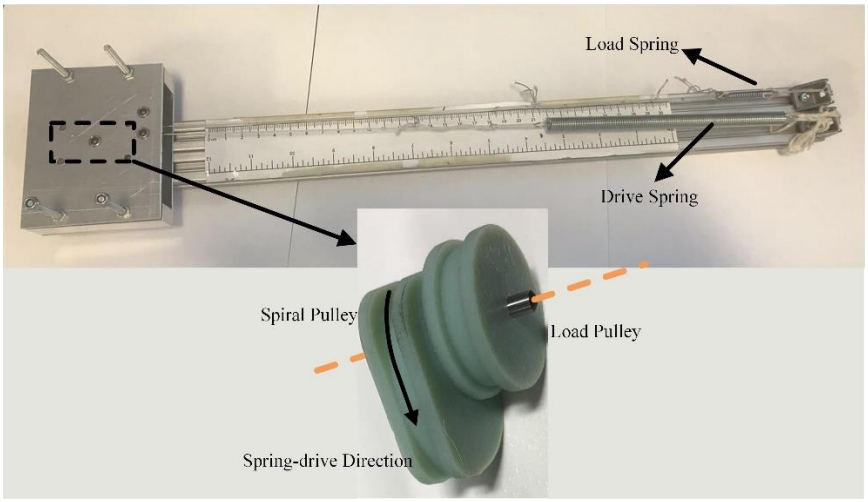

Figure 1. Spiral pulley negative stiffness mechanism [23].

Although this kind of wrapping cam mechanism can provide a satisfactory output torque by choosing the corresponding cam profile [25], the actuation direction is limited by the pulley. Therefore, to develop a negative stiffness mechanism for bidirectional morphing actuation, a bidirectional torsional shaft system is investigated to verify the possibility of a bidirectional energy balancing system. This research focuses on a new negative stiffness mechanism, which is capable of generating a satisfactory torque versus rotation profile. One important benefit of this negative stiffness device is that it is passive and does not require additional energy input for actuation. Energy used in an actuator is usually non-recoverable, but the negative stiffness mechanism can provide energy to actuate and then be back-driveable by the elastic load in the system. Therefore, the coupled system is able to recycle energy and for a conservative system this recycling will be perfectly efficient. This is valuable for morphing structures where the structures have to support significant loads during frequent actuation.

This paper is organised as follows. First, a recent active camber concept is chosen as the target shape adaptive blade, and the required torque in real work conditions is presented [26–28]. The kinematics of the bidirectional torque shaft and rotation angle are then investigated. The active camber device is considered as a general positive stiffness system, and the characteristics of the negative stiffness mechanism is proposed. Finally, the design parameters are optimised to exactly match the requirements of the morphing actuation. The predicted torque, required energy and evolution of efficiency of the coupled system are shown numerically.

2. Morphing aircraft actuation

In order to investigate how to use this bidirectional negative stiffness mechanism for morphing aircraft actuation, a new morphing concept known as the Fish Bone Active Camber (FishBAC) [26] is chosen as the drive load for study. This concept presents a biologically inspired internal bending beam with a skin surface made of elastomeric matrix composite, which can be seen in Fig. 2 [26]. The benefit of this active camber device is that it can provide large camber changes and the airfoil camber

is morphed smoothly and continuously. The rotation of the tendon spooling pulley wraps the tendon to morph the trailing edge upward or downward and produce a continuous change of the camber.

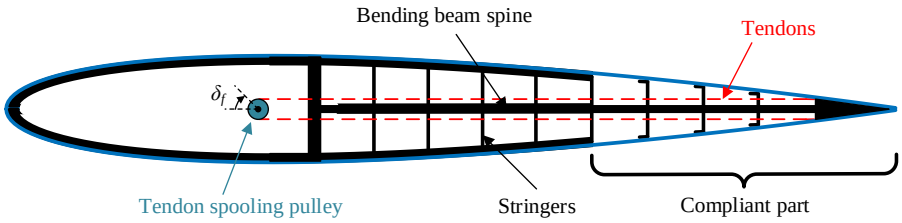

Figure 2. Schematic of the FishBAC concept [26].

In this case, both the aerodynamic load and the elastic deformation of the structure were considered and the analytical formulation was derived from Euler-Bernoulli beam theory. This FishBAC camber is predicted to generate the largest lift coefficient of $C_l = 1.46$ when fully downward deflected, which produces a vertical trailing-edge displacement of $w_e = 14\text{mm}$ (5.2% of chord) and a tendon pulley rotation of $\delta_f = 50$ deg, as shown in Fig. 3.

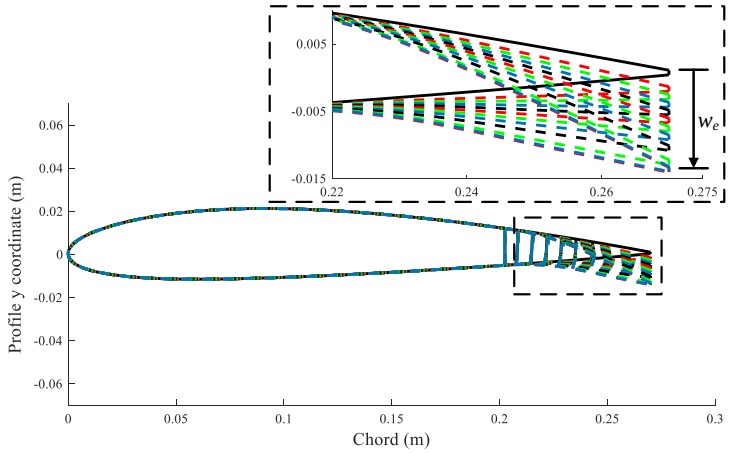

Figure 3. The morphing deformation of the FishBAC model.

Figure 4 shows the predicted bidirectional torque requirements for morphing for different tendon spooling pulley rotation angles. The maximum torque required is 17.4 Nm for elastic deformation at the maximum rotation of $\delta_a = \pm 50$ deg of the spooling pulley. The linearisation of the required torque for morphing produces a target positive stiffness system for designing the bidirectional negative stiffness mechanism.

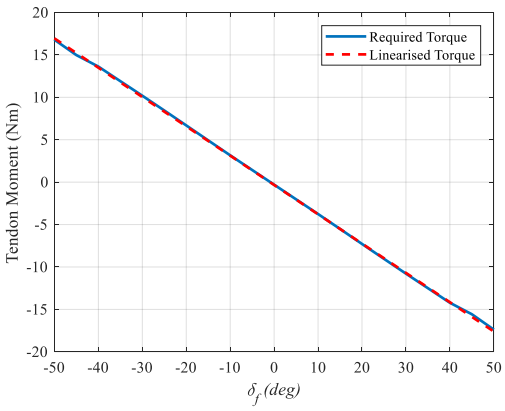

Figure 4. Comparison of required torque and the corresponding linearised torque for elastic deformation.

To allow for a suitable negative stiffness mechanism, it is necessary to simplify the design and assembly. A torsional negative stiffness with an off centre spring (TNSOCS) mechanism is developed to allow the FishBAC to deform either upward or downward. In order to construct an energy balanced system, the extension of a linear spring is used to store energy and installed at the off centre point of the shaft to produce part of the actuating force. Along with the rotation of the regular pulley, a portion of the spring will be released and the moment arm produced by the angle of the bidirectional torque shaft will be increased. Therefore, a negative stiffness mechanism can be designed by careful choice of the system parameters. In order to improve the performance of the total system, a gear is also proposed as an additional parameter. The benefit of using the gear is to provide the ability to modify the gear ratio (G) between the input and output. The schematic of the whole system is shown in Fig. 5, for motion from an initial configuration to an actuated configuration.

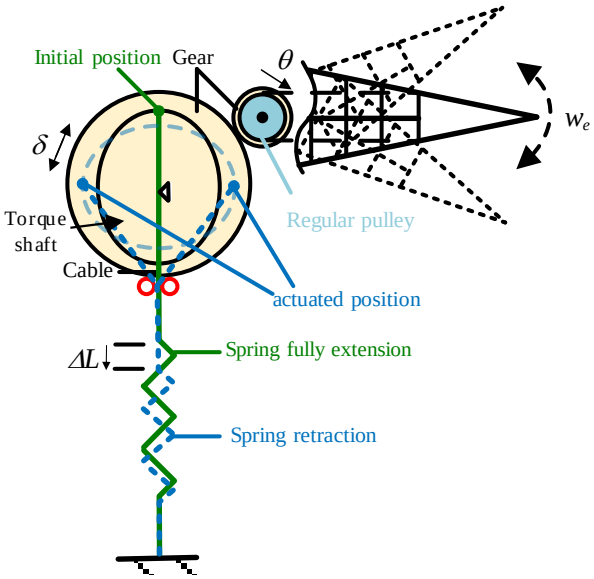

Figure 5. Schematic of the bidirectional negative stiffness mechanism for morphing aircraft actuation.

Figure 6 shows a 3D schematic of the bidirectional shaft concept, which is constructed by a rotation shaft and a load pulley. One side of the prearranged extension spring is installed at an off centre point c on the shaft and the other side is fixed so that can provide a bidirectional motion by rotating the shaft clockwise (B) or anticlockwise (A) around the centre point o. The load pulley is fixed with the bidirectional shaft to output the actuation torque. This bidirectional feature provides better work cancellation for the many practical applications where the required force is bidirectional than single directional devices.

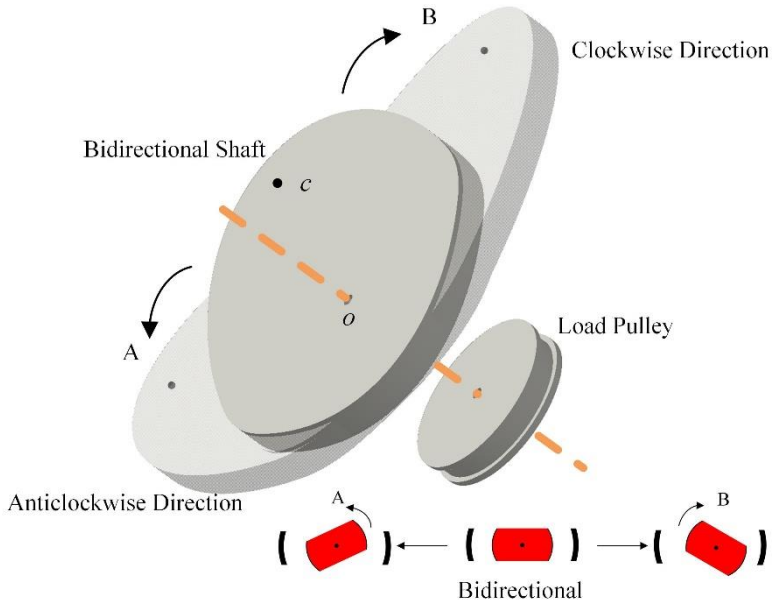

Figure 6. 3D schematic of the bidirectional shaft concept.

3. Bidirectional negative stiffness mechanism

The analysis of a spring-drive FishBAC morphing airfoil employing the bidirectional torque shaft, which is shown in Fig. 5, will be presented. The complicated kinematics of the bidirectional torque shaft and tendon are first investigated, as shown in Fig. 7. The work presented here does not consider practical issues or stability, such as non-backdriveablility, friction, and brakes, in any detail but these important practical aspects will be considered in future work.

The detailed geometry definition of the bidirectional torque shaft is shown in Fig. 7. The bidirectional torque shaft is first defined as an ellipse shaft profile in the Cartesian coordinates about the centre of rotation O and δ is shaft rotation angle. Any profile of the shaft can be adopted to provide a variation of the radius and the ellipse is used here as an example to show how the geometry is able to produce a negative stiffness.

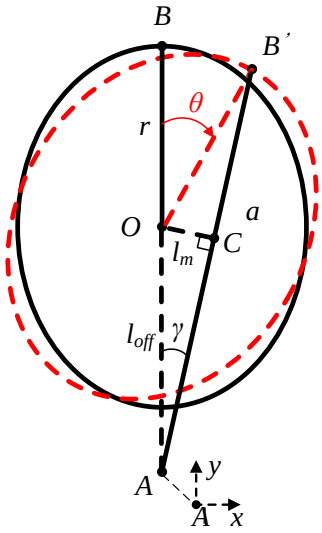

Figure 7. Bidirectional shaft geometry analysis with moment arm details.

Figure 7 shows that the cable is fixed on the shaft and point B is the off centre point for the spring. The Cartesian coordinates can then be defined with the origin point at A and the coordinates of any point B' can then be defined as

$$x_B = r\,sin\,\theta \tag{1}$$

$$y_B = l_{off} + r\cos\theta \tag{2}$$

where r is the length of the vector $\overline{OB}$ and l_{off} is the length of the vector $\overline{OA}$. Therefore, the length of the vector $\overline{AB'}$ is equal to

$$a = \sqrt{x_B^2 + y_B^2} = \sqrt{(r\,sin\,\theta)^2 + \left(l_{off} + r\cos\theta\right)^2} \tag{3}$$

Then, the moment produced by the force in the cable is variation due to change of the moment arm $\overline{OC}$, which is defined as l_m, the length of the vector perpendicular to the straight cable $\overline{AB'}$. The moment arm angle γ can be obtained by using the law of cosines with the known a, r and l_{off}, and is given by

$$\gamma = cos^{-1}\left[\frac{a^2 + l_{off}^2 - r^2}{2al_{off}}\right] \tag{4}$$

The length l_m of the moment arm $\overline{OC}$ is then

$$l_m = l_{off}\,sin\,\gamma \tag{5}$$

Therefore, the total length of the cable from point A to point B' is equal to

$$L_\theta = a \tag{6}$$

Since the length of the cable between the bidirectional torque shaft and the extension spring is essentially constant, the rotation of the bidirectional torque shaft leads to a release of a portion of the cable. The change of the spring force can be calculated by subtracting the total cable length evaluated at each shaft rotation angle θ, from the total cable length at the initial position

$$\Delta L = \left(r + l_{off}\right) - L_\theta \tag{7}$$

The spring is designed as an energy stored device by choosing an initial length L_0 as mentioned above. The force F_s in the spring at the current position can therefore be obtained as

$$F_s = K(L_0 - \Delta L) \tag{8}$$

where K is the spring constant. Finally, the torque produced by the bidirectional torque shaft can then obtained by Eq. (7) and Eq. (5) for each rotation angle θ as

$$T_n = F_s l_m \tag{9}$$

These two independent systems are connected by a gear, as shown in Fig. 5, and the torque T_f on the FishBAC tendon spooling pulley is modified by the gear ratio G to give

$$T_f = T_n G = F_n l_m G \tag{10}$$

and the corresponding rotation of the FishBAC tendon spooling pulley is modified as

$$\delta_f = \frac{\theta}{G} \tag{11}$$

The above discussion shows that as the length of the spring decreases with rotation, the force available from the spring decreases but the magnitude of the moment arm increases. In order to determine the suitable range of the gear ratio, the largest rotation angle of the bidirectional negative stiffness mechanism should be chosen. From the geometry shown in Fig. 8, the largest rotation angle of the bidirectional negative stiffness mechanism occurs when point B' has the maximum corresponding angle γ. Meanwhile, the value of angle γ could be considered as a function of variable θ, and the maximum corresponding angle γ can therefore be solved by differentiating Eq. (4) with respect to θ and setting the result equal to 0. Thus

$$\left.\frac{d\gamma}{d\theta}\right|_{\max\theta} = 0 \tag{12}$$

Therefore, the maximum corresponding angle γ occurs when the vector $\overline{AB'}$ is tangent to a circle with radius of r, as shown in Fig. 8. Equation (13) defines the maximum corresponding angle γ with r, and

the maximum gear ratio can be confirmed by the maximum corresponding angle γ to provide a suitable optimisation upper bound of gear ratio G.

$$\gamma_{max} = sin^{-1}\frac{r}{l_{off}} \tag{13}$$

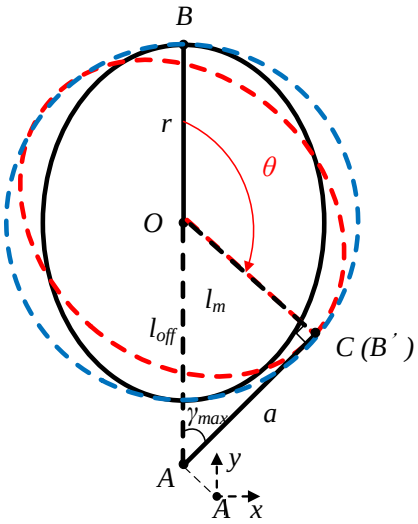

Figure 8. Position corresponding to the maximum angle γ.

In order to minimise the performance of the energy balancing system, an objective energy conversion efficiency function is proposed to make the torque provided by the negative stiffness system match, as closely as possible, the required torque. To accomplished this, an energy conversion efficiency metric is defined as

$$\eta_{ef} = \frac{E_o}{E_r} \tag{14}$$

where E_o is the absolute energy integrates the torque between these two systems

$$E_o = \int_0^{\delta_f} |T_n|\, d\theta \tag{15}$$

and E_r is the required energy for morphing the FishBAC active camber

$$E_r = \int_0^{\delta_f} |T_r|\, d\theta \tag{16}$$

Finally, the nonlinear programming solver *fmincon* in MATLAB Global Optimization Toolbox was used to optimise the objective function. The resulting optimised parameters are shown in Table 1 and the corresponding geometry is shown in Fig. 9.

Table 1. Optimised parameters for bidirectional negative stiffness mechanism optimisation.

Parameter	Lower bound	Upper bound	Optimized value	Units
Drive spring extension, L_0	1/1000	1	0.537	m
Distance, l_{off}	1/1000	3/10	0.292	m
Bidirectional shaft radius, r	1/1000	3/10	0.245	m
Drive spring rate, K	100	1400	1087.392	N/m
Gear ratio, G	0.5	G_{max}	0.522	-

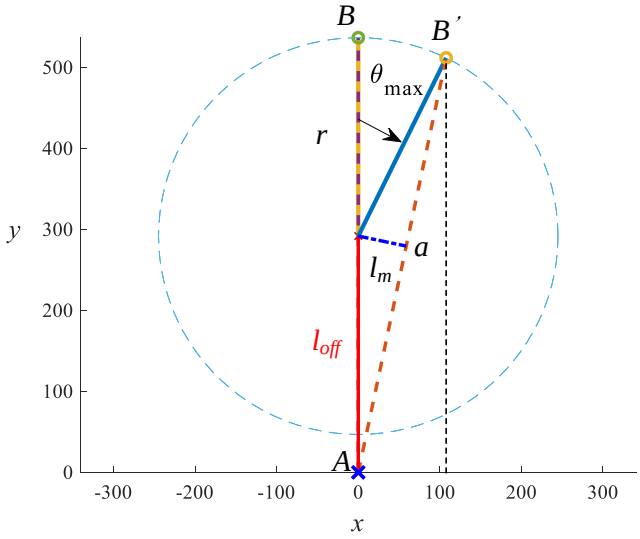

Figure 9. Predicted geometry of the optimised bidirectional pulley.

4. Simulation results and discussion

With the optimised parameters obtained as discussed in Section. 3, the effectiveness of the optimal bidirectional negative stiffness mechanism to construct an energy balancing system for the positive stiffness FishBAC active camber device can be investigated. The performance predicted for the optimised bidirectional torque shaft profile shows satisfactory matching of the linearised torque requirements. Figure 10 shows that the evolution of torque with rotation for the spring and the FishBAC and the net torque of the whole system. The torque provided by the negative mechanism matches the torque required closely, and the maximum torque required by the extra actuator is less than $1\mathrm{N}\cdot\mathrm{m}$.

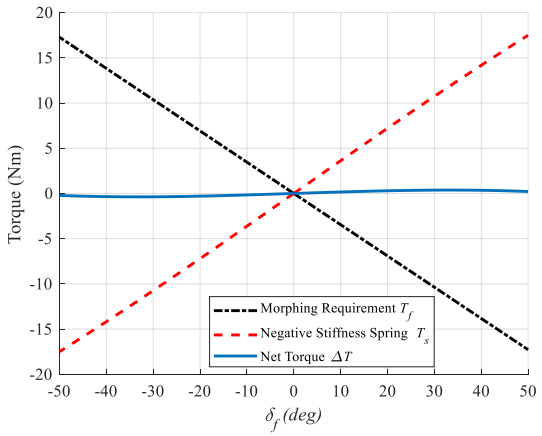

Figure 10. Predicted torque with optimised bidirectional negative stiffness mechanism.

Integrating both the torque (T_f and $\Delta T\left(T_f - T_r\right)$) versus the rotation angle provides the mechanical energy required to morph the FishBAC, as plotted in Fig. 11. By comparing the energy required with and without the negative stiffness mechanism, it shows that the negative stiffness mechanism has a strong ability to passively balance the required torque. Figure 11 shows that the predicted energy reduction is almost 99%, with the energy required reduced from 7.82 J to 0.06 J. This is the contribution of the energy stored in the extended spring in the initial position.

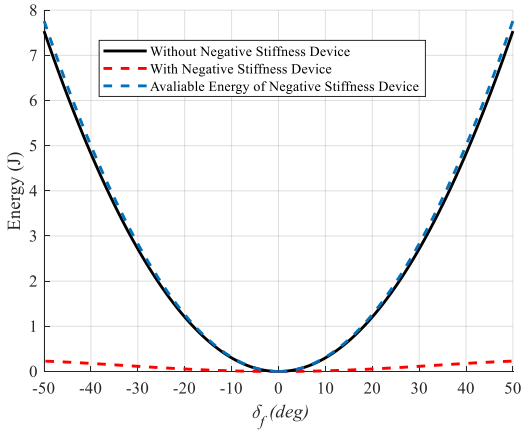

Figure 11. Comparison of predicted energy required with and without the negative stiffness mechanism.

Figure 12 shows the force available from the spring along with the moment arm provided by the negative stiffness mechanism. It can be seen that while the force available from the spring decreases with rotation, the magnitude of the moment arm increases faster. Hence the bidirectional torque varies because of the changing moment arm length when the rotation angle increases, so that the required balancing torque can be produced.

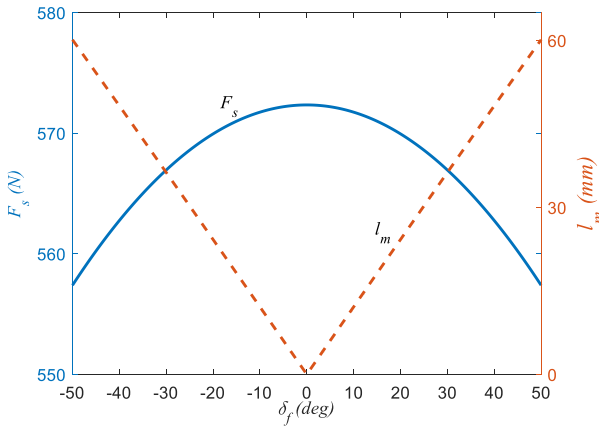

Figure 12. Evolution of the drive spring force with moment arm details.

The objective energy conversion efficiency curve plotted in Fig. 13 shows that the optimised configuration of the bidirectional torque shaft provides significant benefits in terms of energy efficiency. Moreover, it also shows that the bigger the angle of rotation, the less initial energy is lost.

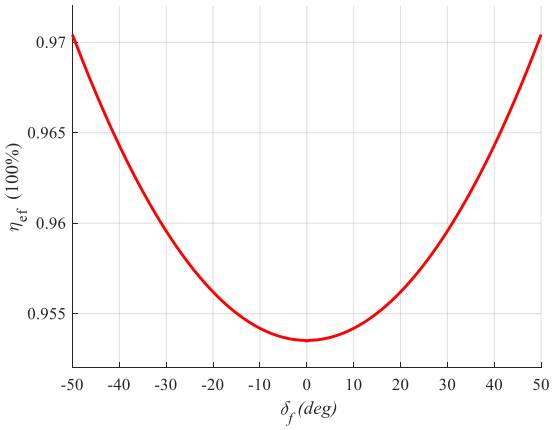

Figure 13. Evolution of efficiency with rotation.

Based on this study, it can be seen that the negative stiffness mechanism provides a significant contribution to balancing the positive stiffness system (FishBAC). High energy conversion efficiency can be provided by the prearranged extension spring and a smaller actuator can be used in the system.

5. Conclusion

A new concept for using a torsional negative stiffness with an off centre spring (TNSOCS) mechanism for bidirectional morphing aircraft actuation has been presented. A bidirectional torque shaft mechanism was proposed as a negative stiffness system by using a pre-tensioned spring. The kinematics of the bidirectional torque shaft mechanism was introduced and this method was used to convert the positive stiffness spring into a negative stiffness system. An energy conversion efficiency function was introduced to provide a basis for evaluation and also act as the objective function to optimise the geometry of the bidirectional negative stiffness mechanism. The optimised bidirectional

torque shaft mechanism was shown to be able to generate a torque that matches to the required torque of the FishBAC active camber closely, which means a significant contribution can be provided by the bidirectional negative stiffness mechanism to balance the positive stiffness system. While the example used in this paper is relatively simple, it provides an insight into the low energy actuation design problem, both in the field of bidirectional morphing aircraft and other fields.

Acknowledgement

This research leading to these results has received funding from the European Commission under the European Union's Horizon 2020 Framework Programme 'Shape Adaptive Blades for Rotorcraft Efficiency' grant agreement 723491.

References

[1] Barbarino S, Bilgen O, Ajaj R M, Friswell M I and Inman D J 2011 A Review of Morphing Aircraft *J. Intell. Mater. Syst. Struct.* **22** 823–77

[2] Barbarino S, Saavedra Flores E I, Ajaj R M, Dayyani I and Friswell M I 2014 A review on shape memory alloys with applications to morphing aircraft *Smart Mater. Struct.* **23** 063001

[3] Li D, Zhao S, Da Ronch A, Xiang J, Drofelnik J, Li Y, Zhang L, Wu Y, Kintscher M, Monner H P, Rudenko A, Guo S, Yin W, Kirn J, Storm S and Breuker R De 2018 A review of modelling and analysis of morphing wings *Prog. Aerosp. Sci.* **100** 46–62

[4] Weisshaar T A 2013 Morphing Aircraft Systems: Historical Perspectives and Future Challenges *J. Aircr.* **50** 337–53

[5] Pontecorvo M E, Barbarino S, Murray G J and Gandhi F S 2013 Bistable arches for morphing applications *J. Intell. Mater. Syst. Struct.* **24** 274–86

[6] Joo J J and Sanders B 2009 Optimal Location of Distributed Actuators within an In-plane Multi-cell Morphing Mechanism *J. Intell. Mater. Syst. Struct.* **20** 481–92

[7] Aguirrebeitia J, Avilés R, Fernández I and Abasolo M 2013 Kinematical synthesis of an inversion of the double linked fourbar for morphing wing applications *Front. Mech. Eng.* **8** 17–32

[8] Wang C, Khodaparast H H and Friswell M I 2016 Conceptual study of a morphing winglet based on unsymmetrical stiffness *Aerosp. Sci. Technol.* **58** 546–58

[9] Wang C, Khodaparast H H, Friswell M I and Shaw A D 2018 Compliant structures based on stiffness asymmetry *Aeronaut. J.* **122** 442–61

[10] Dimino I, Amendola G, Di Giampaolo B, Iannaccone G and Lerro A 2017 Preliminary design of an actuation system for a morphing winglet *2017 8th International Conference on Mechanical and Aerospace Engineering, ICMAE 2017* pp 416–22

[11] Vos R, Barrett R, Breuker R De and Tiso P 2007 Post-buckled precompressed elements: A new class of control actuators for morphing wing UAVs *Smart Mater. Struct.* **16** 919–26

[12] Vos R, Breuker R De, Barrett R M and Tiso P 2007 Morphing Wing Flight Control Via Postbuckled Precompressed Piezoelectric Actuators *J. Aircr.* **44** 1060–8

[13] Tawfik S A, Stefan Dancila D and Armanios E 2011 Unsymmetric composite laminates morphing via piezoelectric actuators *Compos. Part A Appl. Sci. Manuf.* **42** 748–56

[14] Lee T and Chopra I 2001 Design of piezostack-driven trailing-edge flap actuator for helicopter rotors *Smart Mater. Struct.* **10** 15–24

[15] Hall S R and Prechtl E F 1996 Development of a piezoelectric servoflap for helicopter rotor control *Smart Mater. Struct.* **5** 26–34

[16] Calkins F T and Mabe J H 2010 Shape Memory Alloy Based Morphing Aerostructures *J. Mech. Des.* **132** 111012

[17] Zhang J, Zhang C, Hao L, Nie R and Qiu J 2017 Exploiting the instability of smart structure for reconfiguration *Appl. Phys. Lett.* **111**

[18] Huber J E, Fleck N A and Ashby M F 1997 The selection of mechanical actuators based on performance indices *Proc. R. Soc. A Math. Phys. Eng. Sci.* **453** 2185–205

[19] Rizzello G, Riccardi L, Naso D, Turchiano B and Seelecke S 2017 An overview on innovative mechatronic actuators based on smart materials *2017 IEEE AFRICON: Science, Technology and Innovation for Africa, AFRICON 2017* pp 450–5

[20] Karnopp D 1995 Active and Semi-Active Vibration Isolation *J. Mech. Des.* **117** 177

[21] Churchill C B, Shahan D W, Smith S P, Keefe A C and McKnight G P 2016 Dynamically variable negative stiffness structures *Sci. Adv.* **2** e1500778–e1500778

[22] Woods B K S, Friswell M I and Wereley N M 2014 Advanced Kinematic Tailoring for Morphing Aircraft Actuation *AIAA J.* **52** 788–98

[23] Zhang J, Alexander S D, Amoozgar M, Friswell M I and Woods B K S 2018 Spiral Pulley Negative Stiffness Mechanism for Morphing Aircraft Actuation *ASME 2018 International Design Engineering Technical Conferences and Computers and Information in Engineering Conference* (ASME) p V05AT08A018

[24] Woods B K and Friswell M I 2016 Spiral pulley negative stiffness mechanism for passive energy balancing *J. Intell. Mater. Syst. Struct.* **27** 1673–86

[25] Tidwell P H, Bandukwala N, Dhande S G, Reinholtz C F and Webb G 1994 Synthesis of Wrapping Cams *J. Mech. Des.* **116** 634

[26] Woods B K, Bilgen O and Friswell M I 2014 Wind tunnel testing of the fish bone active camber morphing concept *J. Intell. Mater. Syst. Struct.* **25** 772–85

[27] Woods B K S, Dayyani I and Friswell M I 2015 Fluid/Structure-Interaction Analysis of the Fish-Bone-Active-Camber Morphing Concept *J. Aircr.* **52** 307–19

[28] Woods B K S and Friswell M I 2015 The Adaptive Aspect Ratio morphing wing: Design concept and low fidelity skin optimization *Aerosp. Sci. Technol.*